Critical properties and acentric factors of ionic liquids

Alireza Shariati[†], Seyedeh-Soghra Ashrafmansouri, Maryam Haji Osbuei, and Bahar Hooshdaran

School of Chemical and Petroleum Engineering, Shiraz University, Shiraz 71345, Iran
(*Received 14 April 2012 • accepted 19 July 2012*)

Abstract−Since most ionic liquids (ILs) decompose before reaching their critical state, the experimental measurement of their critical properties are not possible. In this study, the critical temperatures, critical pressures and acentric factors of ten commonly investigated ILs were determined by making an optimum fit of the calculated vapor-liquid equilibrium data of binary mixtures of CO_2+IL to the experimental values found in literature. For this purpose, the Peng-Robinson equation of state (PR EoS) and the differential evolution optimization method were used. The ILs considered were 1-ethyl-3-methylimidazolium hexafluorophosphate ([emim][PF_6]), 1-ethyl-3-methylimidazolium bis(trifluoromethylsulfonyl) imide ([emim][Tf_2N]), 1-butyl-3-methylimidazolium tetrafluoroborate ([bmim][BF_4]), 1-butyl-3-methylimidazolium hexafluorophosphate ([bmim][PF_6]), 1-butyl-3-methylimidazolium bis(trifluoromethylsulfonyl) imide ([bmim][Tf_2N]), 1-hexyl-3-methylimidazolium tetrafluoroborate ([hmim][BF_4]), 1-hexyl-3-methylimidazolium hexafluorophosphate ([hmim][PF_6]), 1-hexyl-3-methylimidazolium bis(trifluoromethylsulfonyl) imide ([hmim][Tf_2N]), 1-octyl-3-methylimidazolium tetrafluoroborate ([omim][BF_4]) and 1-octyl-3-methylimidazolium hexafluorophosphate ([omim][PF_6]). To evaluate the ability of the determined parameters in predicting the phase behavior of systems other than the systems that were used for parameter optimization, both sets of parameters obtained in this work and that of Valderrama et al. were used to predict bubble-point pressures of CHF_3+[bmim][PF_6] (by using the PR EoS and the Soave-Redlich-Kwong equation of state. The bubble-point pressures of CO_2+IL systems optimized in this study by the PR EoS were also determined using the Soave-Redlich-Kwong equation of state (SRK EoS). In addition, liquid densities of pure ILs were predicted using a generalized correlation proposed by Valderrama and Abu-Shark. In all cases, the various predicted properties of these ten ILs, were in better agreement with the experimental data, using the critical properties and acentric factor obtained in this study, compared to the values suggested by Valderrama et al.

Key words: Ionic Liquid, Physical Properties, Critical Properties, Critical Temperature, Critical Pressure, Acentric Factor, Modeling, Optimization Method, Differential Evolution

INTRODUCTION

Chemical industries are under pressure to modify or replace many existing processes with technologies having renewable resources and approaching zero pollutant emissions [1]. Such environmental concerns call for new technologies. The substitution of commercial organic solvents by new compounds is among the suitable methods to minimize these problems. Hence, today's world is paying growing attention to green solvents such as room temperature ionic liquids (ILs). One of the most important advantages of ILs is their very low vapor pressures. Because of their insignificant vapor pressures, they pollute neither the working air-environment nor the vapor phase in any process involving both vapor and liquid, including for example, reactions or separations.

ILs are organic salts consisting of organic cations and organic or inorganic anions. In the structure of ILs, the cations are large and asymmetric but the anions are smaller and more symmetric. Due to this high asymmetry in their structure, the packing of ions in a compact lattice is very difficult and hence their melting point is low and they have a wide liquidus range (about 300 °C). These salts are even liquid at ambient temperatures, and therefore, are also called room temperature ILs. This behavior is in contrast to conventional

salts such as sodium chloride. Sodium chloride has a compact lattice because of its symmetric structure and therefore its melting point is high (about 800 °C) [3,4].

In addition to having very low vapor pressures, most ILs are not flammable and have high thermal, chemical and electrochemical stability [5,6]. They are good solvents for both organic and inorganic materials, and polar and non-polar components. This makes them suitable for catalysis [7,8]. Also, they can be designed to have desired characteristics. It is estimated that 10^{18} ILs can be designed by combining various kinds of cations and anions [9,10]. ILs can be used in catalytic reactions, gas drying, gas separations, and liquid-liquid extractions. Moreover, they can be used as electrolytes, lubricants and heat transfer fluids [10-20].

After using an IL as the solvent in a separation process, it is often possible to separate the solute from the IL by extraction with supercritical carbon dioxide without detectable IL contamination. This is because the solubilities of ILs in carbon dioxide are negligibly low [1]. In this respect, ILs have great potential for substituting commercial organic solvents. In current extraction processes, since the solvents usually dissolve in both of the extract and raffinate phases, further separation steps are necessary [21].

Although some experimental data on the phase behavior of various systems containing ILs are available in literature, additional data is often necessary for reliable process design. Such experimental measurements are often difficult, time-consuming, and expen-

[†]To whom correspondence should be addressed.
E-mail: shariati@shirazu.ac.ir

sive. Therefore, it is highly desirable to develop predictive methods for estimating the properties of such systems over a wide range of conditions [2]. Many of the popular models for determining the phase behavior of ILs in various systems require knowledge of the critical temperature, critical pressure and acentric factor of ILs. This includes, for example, many equations of state; however, the critical properties of ILs usually cannot be determined experimentally because most of these compounds start to decompose as temperatures approach their normal boiling points [22]. Since there is no access to the experimental critical temperature and pressure of most ILs, optimization and group contribution methods can be used to estimate these properties. In 2007 and 2008, Valderrama et al. [22,23] estimated these parameters for 250 ILs using a group contribution method based on the concepts of Lydersen [24] and of Joback and Reid [25]. Although in the absence of any data, this method provides critical values for use in equations of state, the shortcoming of using group contribution methods is that, if these methods are used for determining the properties of ILs which were not involved in obtaining the group parameter values, they may not give very accurate results.

In this study, the critical temperatures (T_c), critical pressures (P_c) and acentric factors (ω) of ten ILs consisting of 1-ethyl-3-methylimidazolium hexafluorophosphate ([emim][PF$_6$]), 1-ethyl-3-methylimidazolium bis(trifluoromethylsulfonyl) imide ([emim][Tf$_2$N]), 1-butyl-3-methylimidazolium tetrafluoroborate ([bmim][BF$_4$]), 1-butyl-3-methylimidazolium hexafluorophosphate ([bmim][PF$_6$]), 1-butyl-3-methylimidazolium bis(trifluoromethylsulfonyl) imide ([bmim][Tf$_2$N]), 1-hexyl-3-methylimidazolium tetrafluoroborate ([hmim][BF$_4$]), 1-hexyl-3-methylimidazolium hexafluorophosphate ([hmim][PF$_6$]), 1-hexyl-3-methylimidazolium bis(trifluoromethylsulfonyl) imide ([hmim][Tf$_2$N]), 1-octyl-3-methylimidazolium tetrafluoroborate ([omim][BF$_4$]) and 1-octyl-3-methylimidazolium hexafluorophosphate ([omim][PF$_6$]) were calculated by an optimization method based on the differential evolution approach using the experimental vapor-liquid equilibrium data of binary CO$_2$+IL systems.

PROCEDURE

The Peng-Robinson equation of state [26] with the van der Waals mixing rules with one adjustable parameter (k_{ij}) [27] was used for calculating bubble points. The program was written in a MATLAB environment and the φ-φ approach (using an equation of state to calculate the fugacity coefficients of the components in both liquid and vapor phases) was used for establishing equilibrium at bubble-point conditions [27]. The procedure involves optimizing the values of critical temperature, critical pressure, and acentric factor simultaneously to minimize the objective function defined by Eq. (1). This objective function is the average absolute deviation percent (AAD%) between calculated and experimental bubble-point pressures of binary CO$_2$+IL systems.

$$\text{Obj. Func.} = \frac{1}{N} \times \sum_{i=1}^{N} \left| \frac{P_{exp.} - P_{calc.}}{P_{exp.}} \right| \times 100 \qquad (1)$$

N is the number of experimental bubble-point pressures and '$P_{calc.}$' and '$P_{exp.}$' denote calculated and experimental values of bubble-point pressure, respectively.

To obtain T_c, P_c and ω for [emim][PF$_6$], [emim][Tf$_2$N], [bmim][BF$_4$], [bmim][PF$_6$], [bmim][Tf$_2$N], [hmim][BF$_4$], [hmim][PF$_6$],

[hmim][Tf$_2$N], [omim][BF$_4$], and [omim][PF$_6$], the experimental bubble-point data of binary mixtures of the above-mentioned ILs with CO$_2$ were used. These literature data were taken from the studies of Shariati and Peters [28], Schilderman et al. [29]; Kroon et al. [30]; Kamps et al. [31]; Raeissi and Peters [32], Costantini et al. [33], Shariati and Peters [34]; Kumelan et al. [35]; Gutkowski et al. [36] and Zhang et al. [37], respectively.

The calculations of critical properties and acentric factors followed an optimization method based on differential evolution. A practical optimization technique should have the following characteristics [38]:

1. Ability to handle non-differentiable, nonlinear and multimodal cost functions.

2. Parallelizability to cope with computation-intensive objective functions.

3. Ease of use, i.e., a small number of control variables to steer the optimization. These variables should also be robust and easy to choose.

4. Reliable convergence, i.e., consistent convergence to the global optimum.

In recent years, evolutionary algorithms are gaining popularity in finding the optimal solution of non-linear multimodal problems encountered in many engineering disciplines. Among the evolutionary algorithms, differential evolution (DE) is a novel optimization method which is an improved version of the genetic algorithm (GA) [39] for faster optimization [40]. It is capable of handling non-differentiable, non-linear and multimodal objective functions. Previous studies have shown that differential evolution is an efficient, effective and robust evolutionary optimization method [41]. This method is significantly faster than other optimization methods of numerical optimization and is more likely to find a function's true global optimum [42]. The DE method has a structure similar to the GA method: First, a generation of the parameters is selected from an accepted range, which is defined at the beginning of the program, and then this generation is improved during various iterations until the objective function reaches an acceptable value. The main differences between DE and GA are in the mutation and crossover structures, which lead to differences in the trial vector structure leading to faster optimizations.

RESULTS

Tables 1 and 2 show values of T_c, P_c and ω optimized by our program, together with the values obtained by Valderrama et al. [22, 23] using a group contribution method. The reported AAD% values, presented in Table 1, have been determined by comparing the calculated bubble-point pressures with the corresponding literature data used for optimization of T_c, P_c, and ω in two cases: when the binary interaction parameter between the IL and CO$_2$ is assumed to be zero (k_{ij}=0) and when the binary interaction parameter between IL and CO$_2$ ($k_{ij}\neq0$) is optimized. Table 1 also includes the values of the optimized k_{ij}'s.

As seen in Table 2 (Valderrama's reported data), in each imidazolium-based family (families with the [BF$_4$], [PF$_6$] and [Tf$_2$N] anions), when the molecular weight increases, the value of T_c increases but P_c decreases. In addition, ω increases in each imidazolium-based family as the asymmetry increases. This behavior is in agreement

Table 1. Critical properties and acentric factors of ILs calculated in this work by the differential evolution optimization method and the PR EoS, plus the k_{ij} values

IL	T_c (K)	P_c (bar)	ω	AAD% in P ($k_{ij}=0$)	AAD% in P ($k_{ij}\neq0$)	k_{ij}
[emim][PF$_6$]	738.56	32.12	0.5961	14.35	6.14	0.074768
[emim][Tf$_2$N]	906.91	29.16	0.4223	13.47	13.15	−0.024097
[bmim][BF$_4$]	863.22	34.57	0.8156	8.28	8.19	0.000389
[bmim][PF$_6$]	730.25	27.16	0.6212	25.46	13.04	0.061990
[bmim][Tf$_2$N]	818.52	23.34	0.4881	11.30	11.25	−0.000959
[hmim][BF$_4$]	725.29	25.17	0.9995	11.84	6.80	0.024005
[hmim][PF$_6$]	720.63	23.04	0.8174	15.32	5.82	0.043629
[hmim][Tf$_2$N]	769.14	19.59	0.7948	13.01	11.63	−0.016876
[omim][BF$_4$]	707.13	20.78	1.2784	10.57	1.23	0.015555
[omim][PF$_6$]	646.28	18.22	0.8414	22.14	11.50	0.064226

Table 2. Critical properties and acentric factors of ILs calculated by Valderrama et al. [22,23] using group contribution

IL	T_c (K)	P_c (bar)	ω
[emim][PF$_6$]	663.5	19.5	0.6708
[emim][Tf$_2$N]	1244.9	32.6	0.1818
[bmim][BF$_4$]	632.3	20.4	0.8489
[bmim][PF$_6$]	708.9	17.	0.7553
[bmim][Tf$_2$N]	1265.0	27.6	0.2656
[hmim][BF$_4$]	679.1	17.9	0.9258
[hmim][PF$_6$]	754.3	15.5	0.8352
[hmim][Tf$_2$N]	1287.3	23.9	0.3539
[omim][BF$_4$]	726.1	16.0	0.9954
[omim][PF$_6$]	800.1	14.0	0.9069

Table 3. AAD% in bubble-point pressures calculated for CO_2+IL systems using the SRK EoS when $k_{ij}=0$ and sets of T_c, P_c and ω values obtained in this work (method 1) and by Valderrama et al. [22,23] (method 2)

CO_2+IL	AAD% in P (method 1) at ($k_{ij}=0$)	AAD% in P (method 2) at ($k_{ij}=0$)
CO_2+[emim][PF$_6$]	13.88	18.01
CO_2+[emim][Tf$_2$N]	13.83	17.46
CO_2+[bmim][BF$_4$]	8.53	41.71
CO_2+[bmim][PF$_6$]	25.11	38.72
CO_2+[bmim][Tf$_2$N]	11.38	21.70
CO_2+[hmim][BF$_4$]	10.88	24.17
CO_2+[hmim][PF$_6$]	15.30	23.15
CO_2+[hmim][Tf$_2$N]	12.44	24.82
CO_2+[omim][BF$_4$]	10.73	19.04
CO_2+[omim][PF$_6$]	23.27	23.97

with general observations on other common compounds. According to Table 1, the reported parameters of this work have similar qualitative trends as organic compounds for P_c and ω, but an inverse trend for T_c where an increase in molecular weight, results in the decrease of T_c. This reducing trend is in agreement with Rebelo et al.'s findings [43]. Rebelo et al.'s work [43] predicted the critical temperatures for imidazolium-based ILs (families with the [BF$_4$], [PF$_6$] and [Tf$_2$N] anions) based on the Eötvos and Guggenheim empirical equations (relations based on the temperature-dependence of surface tension and liquid density). By using these equations, they first determined the normal boiling temperatures of ILs. Then, they assumed that the ratio of normal boiling temperature to critical temperature is equal to 0.6 and estimated the critical temperature.

Since experimental data are not available for the calculated properties for comparison, in order to evaluate the values obtained, they

Table 4. AAD% in bubble-point pressure calculated for CO_2+IL systems using the SRK EoS when $k_{ij}\neq0$ and k_{ij} parameters obtained in this work (method 1) and by Valderrama et al. [22,23] (method 2)

CO_2+IL	AAD% in P (method 1) at ($k_{ij}\neq0$)	AAD% in P (method 2) at ($k_{ij}\neq0$)	k_{ij} (method 1)	k_{ij} (method 2)
CO_2+[emim][PF$_6$]	6.02	11.72	0.075955	0.119289
CO_2+[emim][Tf$_2$N]	13.07	14.00	−0.011047	−0.030310
CO_2+[bmim][BF$_4$]	8.22	15.10	−0.004315	0.118232
CO_2+[bmim][PF$_6$]	13.13	13.46	0.061824	0.124923
CO_2+[bmim][Tf$_2$N]	11.32	12.45	−0.004390	−0.047400
CO_2+[hmim][BF$_4$]	7.00	8.87	0.024001	0.096481
CO_2+[hmim][PF$_6$]	6.04	7.19	0.044108	0.090260
CO_2+[hmim][Tf$_2$N]	11.49	15.73	−0.012694	−0.043190
CO_2+[omim][BF$_4$]	10.14	9.33	0.013056	0.063639
CO_2+[omim][PF$_6$]	12.46	13.05	0.037635	0.051615

are used as input parameters to model other properties for which experimental data are available. In this respect, the values of T_c, P_c and ω of this study, as well as Valderrama et al.'s parameters [22, 23] were used to predict the bubble-point pressures of binary CO_2+ IL systems using the SRK EoS (with the van der Waals mixing rules, without the use of any adjustable parameters (k_{ij}'s=0)) instead of the PR EoS, which was used in the optimization process. Although the data set used in this step is the same as that used in the optimization process, the change in the thermodynamic model from PR EoS to SRK EoS [44] is for providing a predictive nature to these calculations. Table 3 shows the AAD% of the bubble-point pressures of both sets of T_c, P_c and ω values (this work and Valderrama et al.'s work [22,23]) for CO_2+IL systems. Table 4 shows these results.

As shown, the results of this work are in better agreement with the experimental data. The average AAD% values from T_c, P_c and ω of this work and Valderrama et al.'s set without considering k_{ij}'s are 14.53% and 25.27%, respectively. If these systems are correlated with the SRK EoS by incorporating k_{ij} values optimized to experimental data, then the average AAD% of this parameter set is only 9.89%, while that of Valderrama et al.'s set is 12.09%. Examples of SRK EoS predictions of bubble-point pressures by this set and that of Valderrama et al. [22,23] are compared for the binary mixture of CO_2+[hmim][PF$_6$] at two different mole fractions of CO_2 in Figs. 1 and 2, with k_{ij}=0. Similar graphs are presented in Figs. 3 and 4 for both parameter sets when k_{ij} is optimized.

In addition, for a fair comparison, the calculated T_c, P_c, and ω of

Fig. 1. Comparison between SRK EoS predictions of bubble-point pressures of CO_2+[hmim][PF$_6$] at x(CO_2)=0.198 and k_{ij}=0 using the parameters obtained in this work and by Valderrama et al. [22,23]. Experimental data are from Costantini et al. [33].
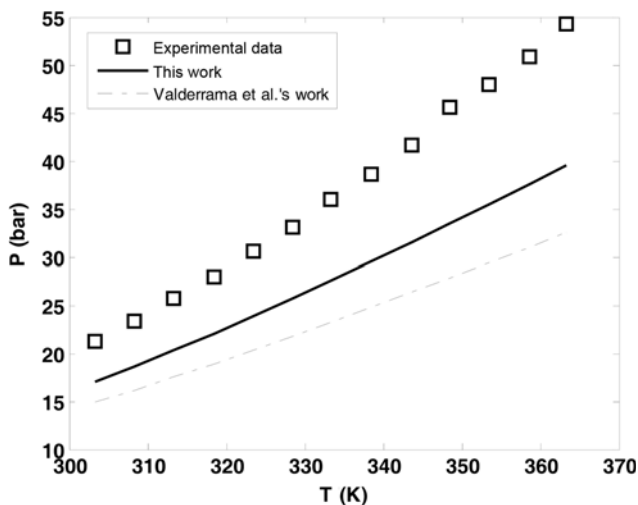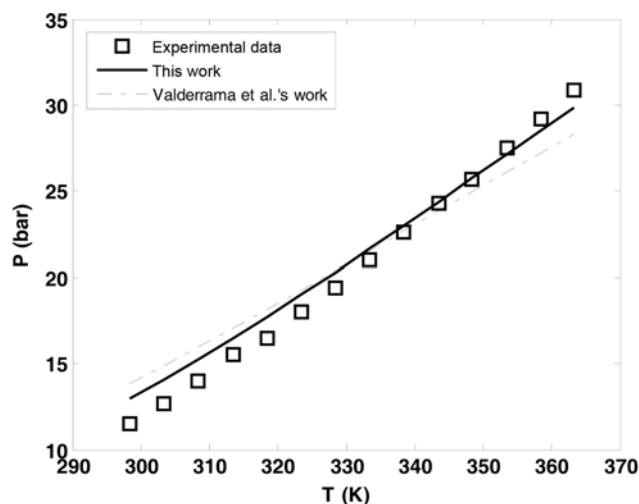

Fig. 3. Comparison between SRK EoS predictions of bubble-point pressures of CO_2+[hmim][PF$_6$] at x(CO_2)=0.198 and $k_{ij}\neq0$ using the parameters obtained in this work and by Valderrama et al. [22,23]. Experimental data are from Costantini et al. [33].
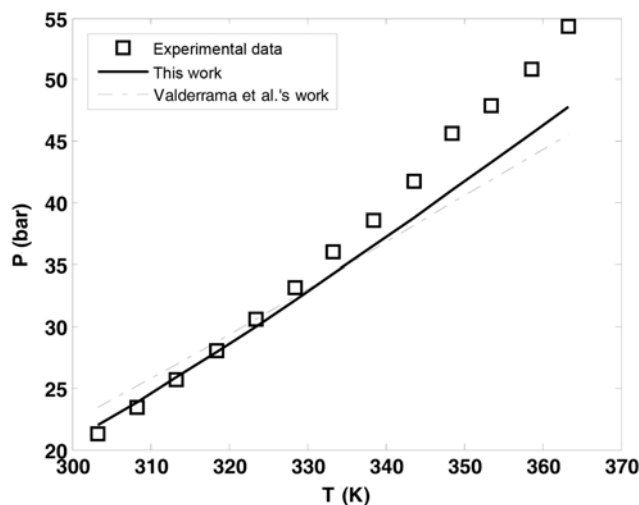

Fig. 2. Comparison between SRK EoS predictions of bubble-point pressures of CO_2+[hmim][PF$_6$] at x(CO_2)=0.299 and k_{ij}=0 using the parameters obtained in this work and by Valderrama et al. [22,23]. Experimental data are from Costantini et al. [33].

Fig. 4. Comparison between SRK EoS predictions of bubble-point pressures of CO_2+[hmim][PF$_6$] at x(CO_2)=0.299 and $k_{ij}\neq0$ using the parameters obtained in this work and by Valderrama et al. [22,23]. Experimental data are from Costantini et al. [33].

Table 5. AAD% in bubble-point pressures calculated for CHF_3+[bmim][PF_6] using SRK EoS and PR EoS by using the parameters obtained in this work (method 1) and by Valderrama et al. [22,23] (method 2), plus the k_{ij} values of each method

	Method 1	Method 2	k_{ij} (method 1)	k_{ij} (method 2)
AAD% in P (PR EoS)	5.97	31.56	0.000000	0.000000
AAD% in P (PR EoS)	1.18	5.66	0.008960	0.068021
AAD% in P (SRK EoS)	1.87	30.85	0.000000	0.000000
AAD% in P (SRK EoS)	1.84	6.045	0.000376	0.069390

this work as well as Valderrama et al.'s work [22,23] are used to predict systems which were not used in our optimization. This consisted of the bubble-point pressures of an IL and a polar gas, namely CHF_3+[bmim][PF_6], using both the SRK EoS and the PR EoS with

the van der Waals mixing rules. The results of these calculations are presented in Table 5 in two cases (k_{ij}=0, k_{ij}≠0). The SRK EoS predictions of the bubble-point pressures of the above-mentioned system using our parameters and those of Valderrama et al. [22-23]
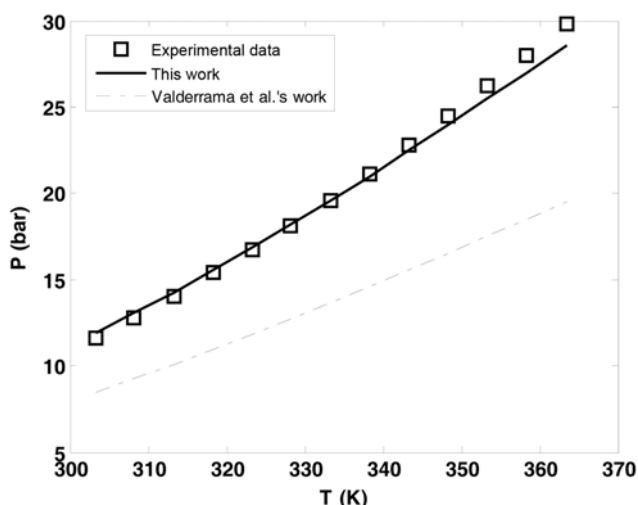

Fig. 5. Comparison between SRK EoS predictions of bubble-point pressures of CHF_3+[bmim][PF_6] at x(CHF_3)=0.102 and k_{ij}= 0 using the parameters obtained in this work and by Valderrama et al. [22,23]. Experimental data are from Shariati and Peters [45].
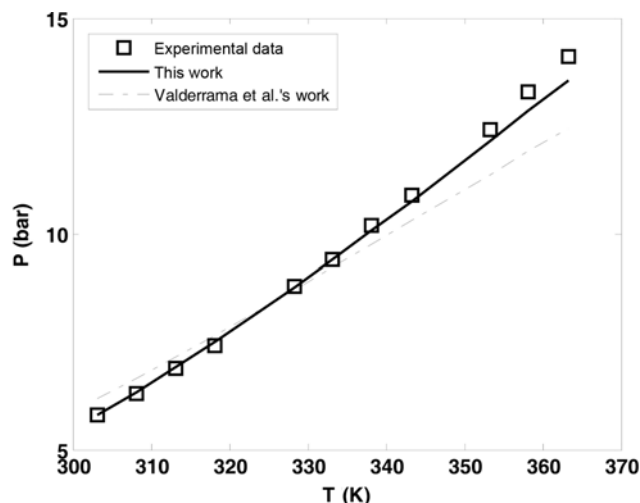

Fig. 7. Comparison between SRK EoS predictions of bubble-point pressures of CHF_3+[bmim][PF_6] at x(CHF_3)=0.102 and k_{ij}≠ 0 using the parameters obtained in this work and by Valderrama et al. [22,23]. Experimental data are from Shariati and Peters [45].
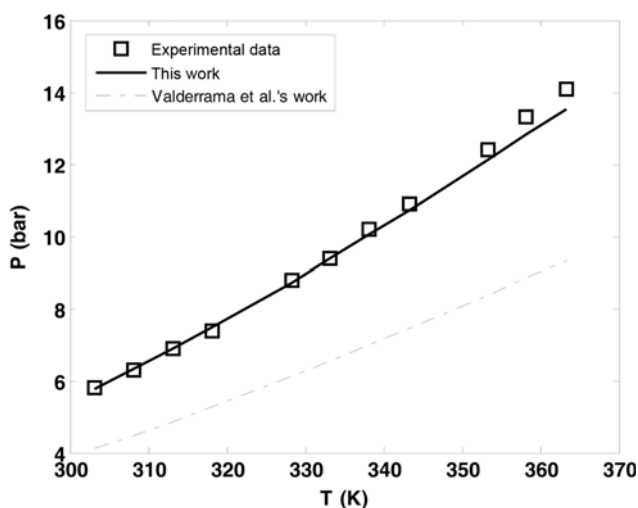

Fig. 6. Comparison between SRK EoS predictions of bubble-point pressures of CHF_3+[bmim][PF_6] at x(CHF_3)=0.203 and k_{ij}= 0 using the parameters obtained in this work and by Valderrama et al. [22,23]. Experimental data are from Shariati and Peters [45].

Fig. 8. Comparison between SRK EoS predictions of bubble-point pressures of CHF_3+[bmim][PF_6] at x(CHF_3)=0.203 and k_{ij}≠ 0 using the parameters obtained in this work and by Valderrama et al. [22,23]. Experimental data are from Shariati and Peters [45].
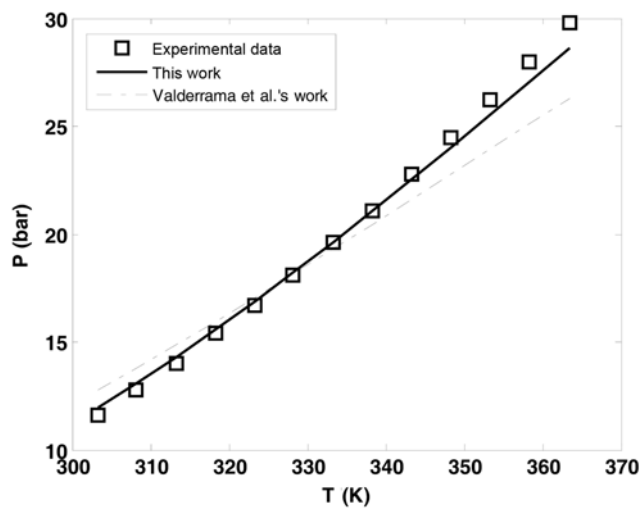
are compared at two different mole fractions of CHF_3 in Figs. 5 and 6 without the use of k_{ij}. Similar graphs are presented in Figs. 7 and 8 when the k_{ij} values are optimized for both parameter sets. The results in this work show better agreement with experimental data in comparison with Valderrama et al.'s reported set [22,23].

The ability of predicting liquid density based on the parameters obtained in this work and Valderrama et al.'s work [22,23] was also investigated by using a generalized liquid density correlation proposed by Valderrama and Abu-Shark [46]. This generalized correlation is based on the equation of Spencer and Danner [47] and requires the reduced temperature at the normal boiling point, the molecular weight, and the critical properties. It is given by the generalized correlation:

$$\rho_L = \frac{MP_c}{RT_c}\left[\frac{0.3445P_c V_c^{1.0135}}{RT_c}\right]^{\Omega} \tag{2}$$

where,

$$\Omega = -\left[\frac{1+(1-T_R)^{2/7}}{1+(1-T_{bR})^{2/7}}\right] \tag{3}$$

Where ρ_L is liquid density in grams per cubic centimeters, M is molecular weight in grams per mole, P_c is critical pressure in bar, V_c is critical molar volume in cubic centimeters per mole, R is the ideal gas constant, T_c is critical temperature in kelvin, T_R is the reduced temperature and T_{bR} is the reduced temperature at the normal boiling point.

Table 6 shows the predicted IL density AAD% values at several temperatures using the above-mentioned generalized correlation with both the property set predicted in this work or by Valderrama [22,23]. The literature liquid density data for [bmim][PF$_6$], [omim][PF$_6$] and [omim][BF$_4$] from Blanchard and Brennecke [48], for [bmim][BF$_4$] and [hmim][PF$_6$] from Gardas et al. [49] and for [emim][Tf$_2$N] from Gardas et al. [50] and Wypych [51]. The literature data of Wypych [51], Letcher and Reddy [52], Kato and Gmehling [53] and Valderrama et al. [22] were used for the liquid density predictions of [bmim][Tf$_2$N], [hmim][BF$_4$], [hmim][Tf$_2$N] and [emim][PF$_6$], respectively. To obtain liquid density by Eq. (2), the normal boiling point values reported by Valderrama et al. [22,23] were used to cal-

culate T_{bR}. The optimized critical parameters obtained in this work succeeded to give better results, also in the case of pure IL density predictions. The difference in the reported AAD% in IL densities reported by Valderrama et al. [22,23] and the predictions of this work is noticeable.

CONCLUSIONS

It is not possible to measure the critical properties of most ILs because they decompose before reaching their critical state. Hence, it is reasonable to use group contribution or optimization methods to obtain the critical properties of ILs.

In this study, the critical temperature, critical pressure and acentric factors of ten ILs have been determined using the differential evolution optimization method coupled with the PR EoS to obtain the best fit of bubble-point pressures of binary CO_2+IL systems. The properties obtained have been compared with the values reported by Valderrama et al. [22,23]. The results show that the parameters of this work can give more accurate predictions of experimental vapor-liquid equilibrium data of binary mixtures of CO_2 and the above-mentioned ILs, as well as CHF_3+[bmim][PF$_6$]. Moreover, the results show that the parameters obtained in this work also predict more accurate pure IL densities in comparison with Valderrama et al.'s parameter set. This success in predicting properties of pure ILs, as well as their binary mixtures, allows for the potential use of these optimized parameters in prediction methods requiring critical properties and acentric factors of ILs as input data.

ACKNOWLEDGEMENTS

NOMENCLATURE

k_{ij} : binary interaction parameter [----]
M   : molecular weight [gr/mole]

Table 6. AAD% in liquid densities calculated for pure ILs at various temperatures and ambient pressure (0.98-1 bar) using the parameters obtained in this work (method 1) and by Valderrama et al. [22,23] (method 2)

IL	Method 1 (T=40 °C)	Method 2 (T=40 °C)	Method 1 (T=50 °C)	Method 2 (T=50 °C)	Method 1 (T=60 °C)	Method 2 (T=60 °C)	Method 1	Method 2
[emim][PF$_6$]	----	----	---	---	---	---	0.065[a]	7.200[a]
[emim][Tf$_2$N]	1.231	2.965	1.032	2.611	0.847	2.282	1.382[b]	3.374[b]
[bmim][BF$_4$]	0.074	5.800	0.0010	6.161	0.016	6.587	---	---
[bmim][PF$_6$]	0.241	5.258	0.319	5.485	0.556	5.864	---	---
[bmim][Tf$_2$N]	---	---	---	---	---	---	0.034[b]	0.600[b]
[hmim][BF$_4$]	---	---	---	---	---	---	0.016[a]	0.600[a]
[hmim][PF$_6$]	0.194	0.792	0.113	0.946	0.003	1.133	---	---
[hmim][Tf$_2$N]	0.025	4.100	---	---	---	---	---	---
[omim][BF$_4$]	0.480	5.138	0.626	4.905	0.782	4.660	---	---
[omim][PF$_6$]	0.102	5.255	0.380	5.033	0.671	4.803	---	---

[a]At 25 °C

[b]At 22 °C

N : number of data point [----]
P : pressure [bar]
P_c : critical pressure [bar]
R : ideal gas constant [$cm^3 \cdot bar/mole \cdot K$]
T_{bR} : reduced temperature at normal boiling point [----]
T_c : critical temperature [K]
T_R : reduced temperature [----]
V_c : critical molar volume [$cm^3/mole$]
x : mole fraction [----]
ρ_L : liquid density [gr/cm^3]
φ : fugacity coefficient [----]
ω : acentric factor [----]

REFERENCES

1. M. C. Kroon, Combined Reactions and Separations Using Ionic Liquids and Carbon Dioxide, PhD Thesis, Printed by Koninklijke De Swart, Printed in the Hague, The Netherlands (2006).
2. M. C. Kroon, E. K. Karakatsani, I. G. Economou, G. Witkamp and C. J. Peters, *J. Phys. Chem. B*, **110**, 9262 (2006).
3. M. J. Earle and K. R. Seddon, *Pure. Appl. Chem.*, **72**, 1391 (2000).
4. P. Wasserscheid and T. Welton, Ionic Liquids in Synthesis, Wiley-VCH Verlag, Weinheim, Germany (2003).
5. M. C. Buzzeo, R. G. Evans and R. G. Compton, *Chem. Phys. Chem.*, **5**(8), 1106 (2004).
6. P. Bonhôte, A. P. Dias, N. Papageourgiou, K. Kalayanasundaram and M. Grätzel, *Inorg. Chem.*, **35**(5), 1168 (1996).
7. H. Olivier-Bourbigou and L. Magna, *J. Mol. Catal. A*, **182-183**, 419 (2002).
8. T. Welton, *Coord. Chem. Rev.*, **248**(21-24), 2459 (2004).
9. C. Chiappe and D. Pieraccini, *J. Phys. Org. Chem.*, **18**, 275 (2005).
10. D. C. Donata, F. Marida and H. Migen, University of Torino (2006). http://lem.ch.unito.it/didattica/infochimica/Liquidi%20Ionici/Definition.html.
11. J. Gorman, *Sci. News*, **160**, 156 (2001).
12. M. R. Ally, J. Braunstein, R. E. Baltus, S. Dai, D. W. DePaoli and J. M. Simonson, *Ind. Eng. Chem. Res.*, **43**, 1296 (2004).
13. J. F. Brennecke and E. J. Maginn, *AIChE J.*, **47**, 2384 (2001).
14. J. G. Huddleston, H. D. Willauer, R. P. Swatloski, A. E. Visser and R. D. Rogers, *Chem. Commun.*, **16**, 1765 (1998).
15. P. Scovazzo, J. Kieft, D. A. Finan, C. Koval, D. DuBois and R. Noble, *J. Membr. Sci.*, **238**, 57 (2004).
16. I. Urukova, J. Vorholz and G. Maurer, *J. Phys. Chem. B*, **109**, 12154 (2005).
17. J. L. Anthony, S. N. V. K. Aki, E. J. Maginn and J. F. Brennecke, *Int. J. Environ. Technol. Manage.*, **4**(1-2), 105 (2004).
18. H. Zhao, S. Xia and P. Ma, *J. Chem. Technol. Biotechnol.*, **80**(10), 1089 (2005).
19. R. Fortunato, C. A. M. Afonso, M. A. M. Reis and J. G. Crespo, *J. Membr. Sci.*, **242**(1-2), 197 (2004).
20. M. Matsumoto, Y. Inomoto and K. Kondo, *J. Membr. Sci.*, **246**(1), 77 (2005).
21. A. Shariati, S. Raeissi and C. J. Peters, CO_2 Solubility in Alkylimidazolium-Based Ionic Liquids, Book Chapter in Developments and Applications in Solubility, Ed. T.M. Letcher, The Royal Society of Chemistry, Cambridge (2007).
22. J. O. Valderrama and P. A. Robles, *Ind. Eng. Chem. Res.*, **46**, 1338 (2007).
23. J. O. Valderrama, W. W. Sanga and J. A. Lazzús, *Ind. Eng. Chem. Res.*, **47**, 1318 (2008).
24. A. L. Lydersen, Estimation of Critical Properties of Organic Compounds. Report 3 University of Wisconsin, College of Engineering, Engineering Experimental Station: Madison, WI (1955).
25. K. K. Joback and R. Reid, *Chem. Eng. Commun.*, **57**, 233 (1987).
26. D. Y. Peng and D. B. Robinson, *Ind. Eng. Chem. Fundam.*, **15**(1), 59 (1976).
27. A. Danesh, PVT and Phase Behaviour of Petroleum Reservoir Fluids, Elsevier B.V. (1998).
28. A. Shariati and C. J. Peters, *J. Supercrit. Fluids*, **29**, 43 (2004).
29. A. M. Schilderman, S. Raeissi and C. J. Peters, *Fluid Phase Equilibria*, **260**, 19 (2007).
30. M. C. Kroon, A. Shariati, M. Costantini, J. V. Spronsen, G. J. Witkamp, R. A. Sheldon and C. J. Peters, *J. Chem. Eng. Data*, **50**(1), 173 (2005).
31. A. P. S. Kamps, D. Tuma, J. Xia and G. Maurer, *J. Chem. Eng. Data*, **48**, 746 (2003).
32. S. Raeissi and C. J. Peters, *J. Chem. Eng. Data*, **54**, 382 (2009).
33. M. Costantini, V. A. Toussaint, A. Shariati, C. J. Peters and I. Kikic, *J. Chem. Eng. Data*, **50**, 52 (2005).
34. A. Shariati, C. J. Peters, *J. Supercrit. Fluids*, **30**, 139 (2004).
35. J. Kumelan, P. S. Kamps, D. Tuma and G. Maurer, *J. Chem. Thermodynamics*, **38**, 1396 (2006).
36. K. I. Gutkowski, A. Shariati and C. J. Peters, *J. Supercrit. Fluids*, **39**, 187 (2006).
37. S. Zhang, X. Yuan, Y. Chen and X. Zhang, *J. Chem. Eng. Data*, **50**(5), 1582 (2005).
38. R. Storn, *J. Global Optimization*, **11**, 341 (1997).
39. D. E. Goldberg, Genetic Algorithms in Search, Optimization, and Machine Learning. Addison-Wesley, Reading, MA (1989).
40. B. V. Babu, P. G. Chakole and J. H. S. Mubeen, *Chem. Eng. Sci.*, **60**, 4822 (2005).
41. B. V. Babu and R. Angira, *Comput. Chem. Eng.*, **30**, 989 (2006).
42. K. Price and R. Storn, *Dr. Dobb's Journal*, **22**, 18 (1997).
43. L. P. Rebelo, J. N. Canongia, J. M. Esperanca and E. Filipe, *J. Phys. Chem. B*, **109**(13), 6040 (2005).
44. G. Soave, *Chem. Eng. Sci.*, **27**, 1197 (1972).
45. A. Shariati and C. J. Peters, *J. Supercrit. Fluids*, **25**, 109 (2003).
46. J. O. Valderrama and B. Abu-Shark, *Fluid Phase Equilib.*, **51**, 87 (1989).
47. C. F. Spencer and R. P. Danner, *J. Chem. Eng. Data*, **17**, 236 (1972).
48. L. A. Blanchard, Z. Gu and J. F. Brennecke, *J. Phys. Chem. B*, **105**(12), 2437 (2001).
49. R. L. Gardas, A. G. M. Ferreira, M. G. Freire, P. J. Carvalho, J. A. P. Coutinho, I. M. Marrucho and I. M. A. Fonseca, *J. Chem. Eng. Data*, **52**, 80 (2007).
50. R. L. Gardas, M. G. Freire, A. G. M. Ferreira, P. J. Carvalho, J. A. P. Coutinho, I. M. Marrucho and I. M. A. Fonseca, *J. Chem. Eng. Data*, **52**, 1881 (2007).
51. G. Wypych, Handbook of Solvents; ChemTec Publishing, Toronto, New York (2001).
52. T. Letcher and P. Reddy, *Fluid Phase Equilib.*, **219**, 107 (2004).
53. R. Kato and J. Gmehling, *J. Chem. Thermodyn.*, **37**, 603 (2005).